JOURNAL OF BIOMOLECULAR STRUCTURE AND DYNAMICS
https://doi.org/10.1080/07391102.2020.1857842

Taylor & Francis
Taylor & Francis Group

1,2,3-Triazole substituted phthalocyanine metal complexes as potential inhibitors for anticholinesterase and antidiabetic enzymes with molecular docking studies

Ümit M. Koçyiğit[a], Parham Taslimi[b], Burak Tüzün[c], Hasan Yakan[d], Halit Muğlu[e] and Emre Güzel[f]

[a]Department of Basic Pharmaceutical Sciences, Sivas Cumhuriyet University, Sivas, Turkey; [b]Department of Biotechnology, Faculty of Science, Bartın University, Bartin, Turkey; [c]Department of Chemistry, Sivas Cumhuriyet University, Sivas, Turkey; [d]Department of Chemistry Education, Ondokuz Mayıs University, Samsun, Turkey; [e]Department of Chemistry, Kastamonu University, Kastamonu, Turkey; [f]Department of Fundamental Sciences, Faculty of Technology, Sakarya University of Applied Sciences, Sakarya, Turkey

Communicated by Ramaswamy H. Sarma

ABSTRACT

In recent years, acetylcholinesterase (AChE) and α-glycosidase (α-gly) inhibition have emerged as a promising and important approach for pharmacological intervention in many diseases such as glaucoma, epilepsy, obesity, cancer, and Alzheimer's. In this manner, the preparation and enzyme inhibition activities of peripherally 1,2,3-triazole group substituted metallophthalocyanine derivatives with strong absorption in the visible region were presented. These novel metallophthalocyanine derivatives (**2-6**) effectively inhibited AChE, with K_i values in the range of 40.11 ± 5.61 to 78.27 ± 15.42 μM. For α-glycosidase, the most effective K_i values of compounds **1** and **2** were with K_i values of 16.11 ± 3.13 and 18.31 ± 2.42 μM, respectively. Also, theoretical calculations were investigated to compare the chemical and biological activities of the ligand (**1**) and its metal complexes (**2**–**6**). Biological activities of **1** and its complexes against acetylcholinesterase for ID 4M0E (AChE) and α-glycosidase for ID 1R47 (α-gly) are calculated. Theoretical calculations were compatible with the experimental results and these 1,2,3-triazole substituted phthalocyanine metal complexes were found to be efficient inhibitors for anticholinesterase and antidiabetic enzymes.

ARTICLE HISTORY
Received 20 October 2020
Accepted 25 November 2020

KEYWORDS
Phthalocyanine; triazole; enzyme inhibition; molecular docking; DFT studies

1. Introduction

Health services are among the most prominent subjects of the 21st century as a result of the increase in the elderly population in the world, prolongation of life expectancy, and socioeconomic changes. With the prolongation of the average life expectancy, the possibility of being exposed to health problems and chronic diseases at later ages increases. Considering these dynamics, while the need for healthcare services increases, innovative drugs will help prevent diseases and reduce treatment costs, so innovative drugs, and treatments will become more and more important in the pharmaceutical industry. Diabetes mellitus is a chronic disease characterized by hyperglycemia, which is a result of insulin resistance and generally accompanying relative insulin insufficiency. Today, it has emerged as a health problem of growing importance because of the frequency and problems all around the world. The prevalence of diabetes mellitus is growing in our country and the world. Due to the high prevalence of diabetes, innovative therapies are needed to provide a healthier life to patients with diabetes (Turkan et al., 2019). The target of diabetes treatment is to normalize the levels of blood glucose and to prevent macro- and microvascular complications. There are different oral antidiabetic agents with different mechanisms of action and different-acting insulins used in type 2 diabetes mellitus treatment (Boztaş et al., 2015). This article will be focusing on the current treatment of type 2 diabetes mellitus.

α-Glycosidase is the enzyme that breaks down oligosaccharides and disaccharides found in brushy edge cells in the small intestine into monosaccharides (Agalave et al., 2011). Acarbose is the only alpha-glucosidase enzyme inhibitor available in our country. There are 50 and 100 mg tablets. It is recommended to take it with the first bite of the meal. Its main side effects are gastrointestinal disorders such as bloating and gas seen in patients. This is when the undigested carbohydrates that reach the lower segments of the intestine are used by the bacterial flora, resulting in gas. Severe diarrhea can be seen in 3% of the cases. This gastrointestinal discomfort can create a tendency to forgo excessive carbohydrate consumption and increase dietary compliance. Also, cholinesterases (ChEs) are considered to be a class of enzymes that catalyze the hydrolysis of acetylcholine (ACh) to choline and acetic acid, a key process for the restoration of cholinergic neurotransmission. Although there are many ongoing research activities for the treatment of Alzheimer's

CONTACT Burak Tüzün btuzun@cumhuriyet.edu.tr Department of Chemistry, Sivas Cumhuriyet University, Sivas, Turkey; Emre Güzel eguzel@subu.edu.tr Department of Fundamental Sciences, Faculty of Technology, Sakarya University of Applied Sciences, Sakarya, Turkey.

Supplemental data for this article can be accessed online at https://doi.org/10.1080/07391102.2020.1857842.

disease, only some medicines such as Tacrine, Donepezil, and Rivastigmine have been approved by the Food and Drug Administration (FDA) (Ismail et al., 2012).

Phthalocyanines (Pcs) and its metal complexes have attracted a lot of attention due to their electronic structure properties and have been recognized as important complexes for many applications in materials science. The properties of phthalocyanines can be modulated by altering their chemical structures by adding different metals that can coordinate to the cavity of the macrocycle and using varying axial and peripheral ligands and substituents. Pc complexes that chemical properties can be changed in these ways, continue to be used in important areas such as electrochromic devices (Güzel et al., 2019b), photosensitizers (Güzel et al., 2013; Ogbodu et al., 2020), solar cells (Yıldız et al., 2019), catalysts (Jiang et al., 2013), heavy metal sensors (Beduoğ lu et al., 2020) and enzyme inhibitors.

The triazole groups are important nitrogen heterocycles that have been extensively investigated to obtain many strong azole fungicides (Tan et al., 2012). Especially in recent years, compounds containing 1,2,3-triazole groups have started to be used in light stabilizers and optical brighteners. 1,2,3-triazole groups have advantages in binding biological molecular targets, such as being stable against metabolic degradation, being able to bind hydrogen, and increasing the solubility of the compound (Dalvie et al., 2002; Sepehri et al., 2020; Seth Horne et al., 2004). Synthetic compounds containing 1,2,3-triazole units have various biological activities and are indispensable as starting compounds for the synthesis of many heterocycles. Compounds with the triazole group have been used as HIV-1 protease inhibitors, human β3-adrenergic receptors, antituberculosis, antinuclear, antibacterial, and anticancer agents (Agalave et al., 2011; Bulut et al., 2018; Güzel, 2019).

In a current conflict, efforts have been made to develop more effective and more active drug molecules. It is seen in these studies that it tries to form a complex with metal atoms to synthesize more effective and active molecules (Günsel et al., 2019; Seth Horne et al., 2004). It is seen in these studies that the metal complexes formed were found to be more effective than ligand molecules. The theoretical and experimental results made also support this situation. Many theoretical methods are used to compare the chemical and biological activities of the studied ligand molecule and its metal complexes. The most important of these methods are calculations made with the gaussian software program and molecular docking calculations. The working ligand and its metal complexes were calculated with the Gaussian software program in HF/6-31G and B3LYP/6-31G basis sets. Then, molecular docking calculations were made to compare the biological activities of the ligand and its metal complexes against the studied enzymes whose name are acetylcholinesterase for pdb ID:4M0E (AChE) (Cheung et al., 2013) and α-glycosidase for pdb ID:1R47 (α-Gly) (Garman & Garboczi, 2004).

Taking these properties into consideration, it has focused on non-aggregate phthalocyanine derivatives as a strategy in conjunction with the 1,2,3-triazole groups to study enzyme inhibitions and theoretical and molecular docking calculations. In the literature, there are few studies in which triazole-substituted phthalocyanines are used as enzyme inhibitors (Arslan et al., 2019a, 2019b; Kantar et al., 2015). α-Glycosidase enzyme inhibition activities of 1,2,3-triazole groups substituted phthalocyanines have not been reported in the literature and this is the first study of 1,2,3-triazole groups substituted phthalocyanines as a potential α-glycosidase enzyme inhibitor. So, we have investigated the inhibition effects of anticholinesterase and antidiabetic enzymes and to record favorable and good AChE and α-glycosidase inhibition properties of these compounds to give directions to further studies.

2. Experimental

2.1. Materials and methods

The used equipment, materials, and application parameters were presented as supplementary information. 4-((1-phenyl-1H-1,2,3-triazol-5-yl)methoxy)phthalonitrile (**1**) and its zinc phthalocyanine derivative (**2**) were prepared according to the reported method (Güzel, 2019).

2.1.1. Synthesis

2.1.1.4. General procedure for the synthesis of the phthalocyanines (2–6). Phthalonitrile derivative (**1**) (0.100 g, 0.36 mmol), anhydrous $ZnCl_2$, $Mn(CH_3COO)_2$, $NiCl_2$, $CuCl_2$, $CoCl_2$ ∼ (0.025 g, excess) in amyl alcohol and 1,8-diazabicyclo[5.4.0]un-dec-7-ene (DBU, 0.05 mL) were heated in sealed tube under an argon atmosphere for 10 h. After, the resulting green mixture was cooled to room temperature. The crude products were precipitated by methanol-water, filtered off, and then washed with the ethanol. The crude products were further isolated by column chromatography utilizing a mixture of THF:EtOH (20:1 v/v) as an eluent.

Yield of **3**: 25.7 mg (24.4%). FT-IR (υ_{max}/cm^{-1}): 3060 (Ar-C-H), 2936-2888 (Aliph. -C-H), 1610 (Ar-C = C), 1502, 1440 (-N = N), 1366 (-C-N) 1230, 1115, 1042, 766, 688. UV-vis λ_{max} (nm) THF: 735, 652, 484, 312. MS (MALDI-TOF): *m/z* 1260.22 $[M]^+$.

Yield of **4**: 30.3 mg (28.8%). FT-IR (υ_{max}/cm^{-1}): 3048 (Ar-C-H), 2936-2855 (Aliph. -C-H), 1544 (Ar-C = C), 1525, 1456 (-N = N), 1366 (-C-N) 1222, 1108, 1042, 752, 691. ^{1}H-NMR (300 MHz, $CDCl_3$): δ, ppm 9.06 (s, 4H, Triazole Ar–H), 8.76-7.52 (32H, m, Pc-Ar-H, and Ar-H), 5.72 (8H, s, OCH_2). UV-vis λ_{max} (nm) THF: 680, 610, 332. MS (MALDI-TOF): *m/z* 1264.12 $[M]^+$.

Yield of **5**: 21.5 mg (20.4%). FT-IR (υ_{max}/cm^{-1}): 3066 (Ar-C-H), 2930-2866 (Aliph. -C-H), 1562 (Ar-C = C), 1512, 1448 (-N = N), 1356 (-C-N) 1232, 1102, 1048, 760, 692. UV-vis λ_{max} (nm) THF: 684, 617, 346. MS (MALDI-TOF): *m/z* 1268.96 $[M]^+$.

Yield of **6**: 23.5 mg (22.4%). FT-IR (υ_{max}/cm^{-1}): 3084 (Ar-C-H), 2926-2852 (Aliph. -C-H), 1578 (Ar-C = C), 1502, 1428 (-N = N), 1344 (-C-N) 1232, 1109, 1036, 744, 698. UV-vis λ_{max} (nm) THF: 673, 604, 308. MS (MALDI-TOF): *m/z* 1264.22 $[M]^+$.

2.1.2. Enzyme inhibition assays

The α-glycosidase inhibitory effect of novel synthesized compounds was examined using *p*-nitrophenyl-D-glycopyranoside (*p*-NPG) as a substrate and the absorbance values were calculated at 405 nm spectrophotometrically (Demir et al., 2020; Genc Bilgicli et al., 2020; Gülçin et al., 2020; Lolak et al., 2020; Tao et al., 2013; Taslimi et al., 2020; Türkan et al., 2020). Several solutions in phosphate buffer (PB) were prepared in case of getting entire enzyme inhibition. First, 75 μL of PB was mixed with 20 μL of the enzyme solution in PB (0.15 U/mL, pH 7.4) and 5 μL of the sample (Bursal et al., 2020). Then it was pre-incubated at 37 °C for 10 min before adding the *p*-NPG to the initiation of the reaction. Also, 50 μL of *p*-NPG in phosphate buffer (5 mM, pH 7.4) after preincubation was added and again incubated at 37 °C. The inhibitory effects of AChE were determined according to the method of Ellman's test (Ellman et al., 1961). Acetylthiocholine iodide (AChI) was used as substrates. 5,5′-Dithiobis (2-nitrobenzoic acid) (Ellman reagent, DTNB) was used to measure AChE activity. Briefly, 50 μL DTNB and 100 μL of Tris–HCl solution (1 M, pH 8.0), 750 mL of sample solution dissolved in distilled water at disparate concentrations, and 50 μL AChE (5.32×10^{-3} U) solution were incubated and mixed for 15 min at 30 °C. Finally, the reaction was started by adding 50 μL of AChI. The hydrolysis of substrates was monitored spectrophotometrically by the formation of yellow 5-thio-2-nitrobenzoate anion as a result of the reaction of DTNB with thiocholine, released by the enzymatic hydrolysis of AChE, at a wavelength of 412 nm (Kocyigit et al., 2018). The inhibition effects of novel synthesized compounds were determined from activity(percent) *versus* synthesized derivatives graphs for each compound (Akbaba et al., 2013; Lolak et al., 2020) with at least five different inhibitor concentrations on α-Gly and AChE. The IC_{50} values were calculated from activity (%) against compound inhibition.

2.1.3. Theoretical methods

2.1.3.1. Gaussian study. It is used to compare the biological and chemical activities of molecules with bioinformatic chemistry. A lot of information about the molecules of the ligand and its metal complexes is obtained by bioinformatic calculations. Using this information, molecules with higher biological and chemical activities and their metal complexes are synthesized. These studied molecules were performed by the Hartree-Fock (HF) and Becke, 3-parameter (Becke, 1988; Stephens et al., 1994), Lee-Yang-Parr (B3LYP) (Hohenstein et al., 2008; Wiberg, 2004) method with 6-31G basis set by Gaussian software program (Frisch et al., 2009). As a result of the calculations made on these basis sets, many parameters can be obtained. HOMO that is Highest Occupied Molecular Orbital and LUMO that is Lowest Unoccupied Molecular Orbital values are used to obtain information about the activities of molecules by using these methods. There are many parameters obtained from quantum chemical calculations and these are called quantum chemical parameters such as E_{HOMO}, E_{LUMO}, ΔE (HOMO-LUMO energy gap), electronegativity (χ), chemical potential (μ), chemical hardness (η), electrophilicity (ω), nucleophilicity (ε), global softness (σ) and proton affinity (PA) (Bitmez et al., 2014).

2.1.3.2. Docking study. There is a method used to compare the biological activities of the ligand and its metal complexes against enzymes. The most common of these is molecular docking. A few of these molecular docking methods can be used to compare metal complexes. In this study, HEX program is used. The ligand and its metal complexes interact with these enzyme proteins to increase their biological activity (Kurtoglu et al., 2014). Molecular docking calculations compared molecules' biological activities against enzymes. *.pdb extension file was created using the structure of the optimized molecule with the Gaussian software program (Frisch et al., 2009). The enzymes and molecule files were studied at HEX 8.0.0 (Ritchie & Venkatraman, 2010). The following parameters are used for docking: correlation type-shape only, FFT mode: 3D, grid dimension: 0.6, receptor range: 180, ligand range: 180, twist range: 360, distance range: 40. Also, Protein-Ligand Interaction Profiler (PLIP) server was used to examine the interaction between protein and the compounds in detail (DeLano, 2002).

3. Results and discussion

3.1. Synthesis and characterization

Figure 1 represents the synthetic route of metallophthalocyanine complexes (**2**–**6**). The reactions were continued utilizing DBU and the anhydrous metal salts ($ZnCl_2$ for **2**, $Mn(CH_3COO)_2$ for **3,** $NiCl_2$ for **4**, $CuCl_2$ for **5**, and $CoCl_2$ for **6**) and appropriate solvents (amyl alcohol) at 140 °C.

The crude complexes were isolated after washing several times with the alcohol/water mixture. The yields obtained for the manganese, nickel, copper and cobalt phthalocyanines (**3–6**) are 24%, 28%, 20%, and 22%, respectively. Elucidation of the novel phthalocyanine complexes was performed with ultraviolet-visible spectrophotometry, elemental analysis, Fourier transform infrared spectrometry (FT-IR), ^{1}H-NMR spectroscopy, and MALDI-TOF mass spectrometry. The FT-IR spectrum of phthalocyanines (**2**–**6**), the -C≡N vibration of compound (**1**) at 2230 cm^{-1} disappeared as expected. Stretching vibrations of aliphatic C-H bonds of phthalocyanines (**3**–**6**), as in the phthalonitrile derivative, were detected at around 2930 cm^{-1}. Similarly, stretching vibrations of aromatic C-H bonds of phthalocyanines (**3**–**6**) were observed at around 3050 cm^{-1}. 1,2,3 Triazole groups have stretching vibrations belonging to –N = N groups, and they appeared around at around 1450 cm^{-1}. Furthermore, the peak at 1352 cm^{-1} of the compound (**2**) containing 1,2,3 triazole group proved the presence of -C-N bonds in the structure^{1}H-NMR investigations of complex **4** provided the expected chemical changes for the structure. ^{1}H-NMR spectra of (**3, 5,** and **6**) were precluded due to their paramagnetic nature (Nas et al., 2017). The wide range of derivatives obtained by MALDI-TOF techniques confirmed the expected structures. Also, it has been found that the complexes synthesized in the structures observed without significant fragmentation are

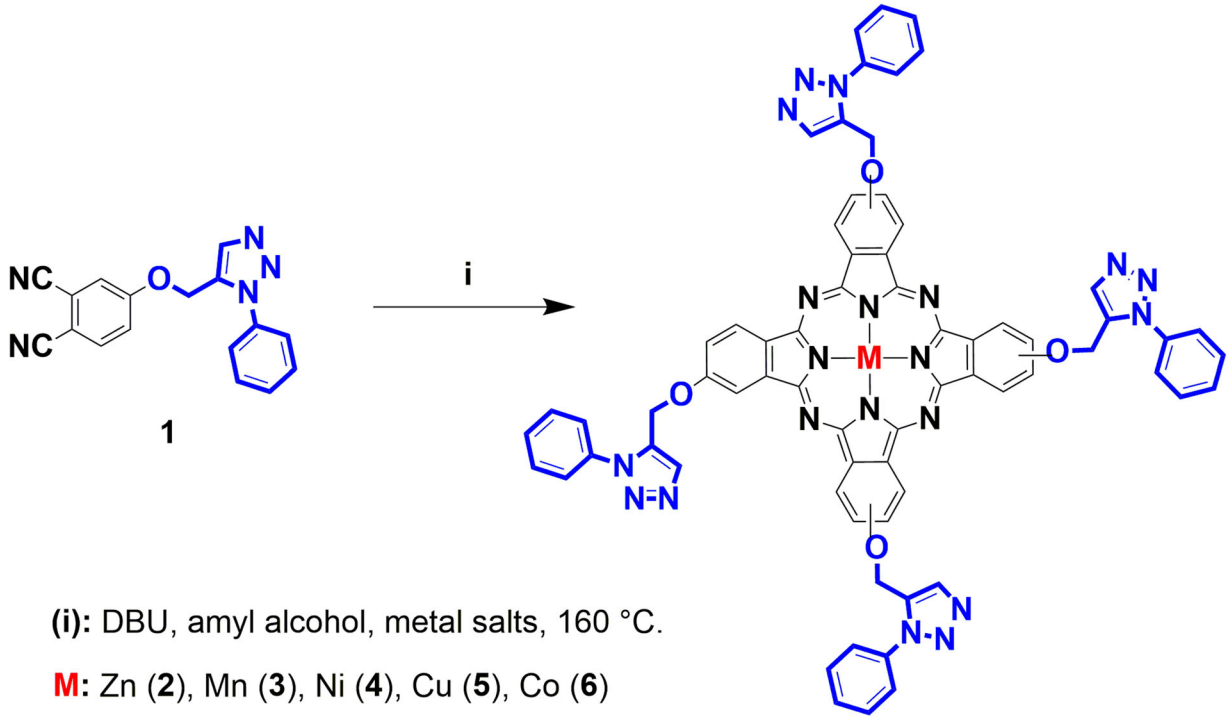

Figure 1. The synthesis of phthalonitrile derivative (**1**) and its metallophthalocyanine complexes (**2–6**).

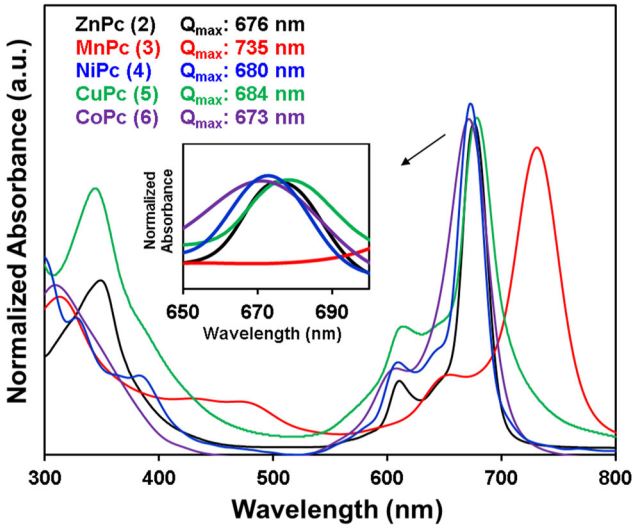

Figure 2. Normalized absorption spectra of the phthalocyanine complexes in THF.

stable under MALDI-MS conditions. The molecular ion peaks were observed at *m/z*: 1260.22 $[M+H]^+$ for **3**, 1264.12 $[M-Cl+H]^+$ for **4**, 1268.96 $[M+H]^+$ for **5** and 1264.24 $[M+H]^+$ for **6**.

3.2. UV-Vis absorption studies

One of the most widely used methods to understand the absorption properties of phthalocyanine complexes is absorption spectroscopy. Phthalocyanines show exclusive electronic spectra in two regions in absorption spectroscopy. One of them is the UV region at about 300–350 nm (B band) and the other in the visible area at 600–700 nm (Q-band) (Güzel et al., 2015). The UV-vis absorption spectra of the metallophthalocyanine complexes (**2-6**) in THF is exhibited in Figure 2. The intense and sharp well-defined Q-band centered at 676 for **2**, 735 nm for **3**, 680 nm for **4**, 684 nm for **5** and 673 nm for **6** exhibits the lack of aggregation phenomena in the solution.

In metallophthalocyanine complexes (**2-6**), the single (narrow) Q bands shown that these phthalocyanines are in monomeric form in the solvent medium. All complexes demonstrated intense single Q-absorption bands which are indicative of the metallophthalocyanines with the D_4h symmetry (Güzel et al., 2020, 2017; Özçeşmeci et al., 2012). Also, manganese phthalocyanine (**3**) exhibits absorption at 484 nm, which was interpreted as a charge transfer absorption (phthalocyanine ring to metal).

3.3. Metabolic enzymes inhibition results

3.3.1. AChE inhibition results

Recently, recording novel inhibitors targeting AChE has still been of significant interest to the researchers. Additionally, it is recorded that selective AChE inhibitors can circumvent classical cholinergic toxicity. Hence, the development of novel selective AChE inhibitor compounds can provide additional benefits in the therapy of AD. Recently, there is a major interest in the extension of selective AChE inhibitors (Bal et al., 2020; Yiğit et al., 2020). All of metallophthalocyanine complexes (**2–5**) had significantly higher AChE inhibitory activity than that of standard AChE inhibitors such as Tacrine. Furthermore, the K_i values of compounds (**1–6**) and are summarized in Table 1. As can be seen from the results obtained in Table 1, these peripherally substituted metallophthalocyanine complexes (**2–6**) effectively inhibited AChE, with K_i values in the range of 40.11 ± 5.6 to 78.27 ± 15.42 μM.

Table 1. The enzyme inhibition results of novel complexes (**1–6**) against acetylcholinesterase (AChE) and α-glycosidase (α-Gly) enzymes.

	IC_{50} (μM)			K_i (μM)		
Compounds	AChE	r^2	α-Gly	r^2	AChE	α-Gly
1	134.21	0.9731	11.65	0.9861	125.35 ± 16.21	16.11 ± 3.13
2	62.54	0.9289	22.21	0.9572	53.24 ± 11.23	18.31 ± 2.42
3	44.31	0.9412	30.01	0.9241	40.11 ± 5.61	38.51 ± 13.55
4	81.38	0.9887	26.18	0.9588	73.62 ± 11.05	26.24 ± 5.96
5	88.78	0.9131	42.14	0.9134	78.27 ± 15.42	40.34 ± 3.28
6	71.52	0.9032	38.56	0.9581	59.71 ± 7.65	48.08 ± 6.40
TAC	128.08	0.9144	–	–	107.21 ± 13.48	–
ACR	–	–	51.45	0.9981	–	48.52 ± 8.08

However, the compound **1** had almost similar inhibition profiles with standard compound (Tacrine, TAC). The most active **3** showed K_i values of 40.11 ± 5.6 μM. For AChE, IC_{50} values of TAC as positive control and some novel compounds were studied in this study the following order: **3** (44.31 μM, r^2: 0.9412)< **2** (81.38 μM, r^2: 0.9887) < **6** (71.52 μM, r^2: 0.9032)< **4** (81.38 μM, r^2: 0.9887)< **5** (88.78 μM, r^2: 0.9132)< **TAC** (128.08 μM, r^2: 0.9144) < **1** (134.21 μM, r^2: 0.9731).

3.3.2. α-Glycosidase inhibition results. Recently, many α-glycosidase inhibitors have been discovered and studied (Erdemir et al., 2019; Taslimi et al., 2017) Anti-diabetic drugs that are used in clinical practice, such as acarbose, voglibose, and miglitol, competitively inhibit α-glycosidase in the brush border of the small intestine which subsequently interrupts hydrolysis of carbohydrate and improves postprandial hyperglycemia. For enzyme glycosidase, compounds (**1–6**) have IC_{50} values in the range of 11.65–42.14 μM and K_i in the range of 16.11 ± 3.13 to 48.08 ± 6.40 μM (Table 1). The results have documented that all of these compounds (**1–6**) have shown the inhibitory effects of α-glycosidase similar to acarbose (IC_{50}: 51.45 μM) as a standard glycosidase inhibitor. The most effective K_i values of **1** and **2** were with K_i values of 16.11 ± 3.13 and 18.31 ± 2.42 μM, respectively. For α-glycosidase, IC_{50} values of ACR as positive control and some compounds (**1-6**) the following order: **1** (11.65 μM, r^2: 0.9861)< **2** (22.21 μM, r^2: 0.9572) < **4** (26.18 μM, r^2: 0.9588)< **3** (30.01 μM, r^2: 0.9241)< **6** (38.56 μM, r^2: 0.9581) < **5** (42.14 μM, r^2: 0.9134) < **ACR** (51.45 μM, r^2: 0.9981). Presently, the management of diabetes involves among others administration of oral hypoglycemic substances such as biguanide, a thiazolidinedione, sulphonylurea, and α-glucosidase inhibitors (He et al., 2015) (Figures 3 and 4).

3.4. Theoretical calculations

Chemical and biological activity values of molecules are calculated with theoretical calculations. With theoretical calculations, many parameters about molecules and their metal complexes are obtained. DFT calculations were made to compare the chemical activities of the ligand molecule and its metal complexes (Akkoç et al., 2020; Güzel et al., 2019a). Many parameters were obtained from these calculations. Among these parameters, the two most important parameters are the numerical value of the HOMO and LUMO energy levels of the molecules. The numerical value of the HOMO

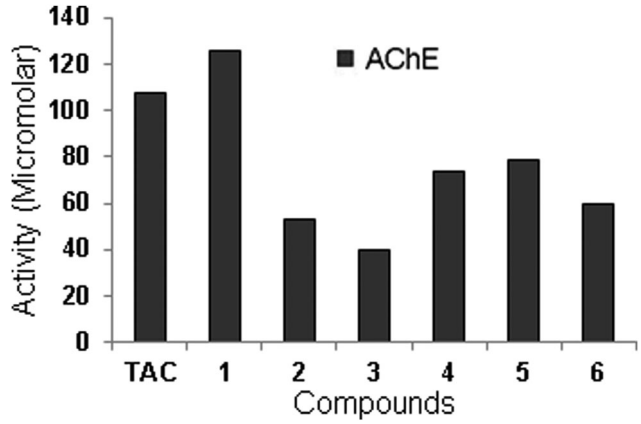

Figure 3. K_i values for AChE enzyme.

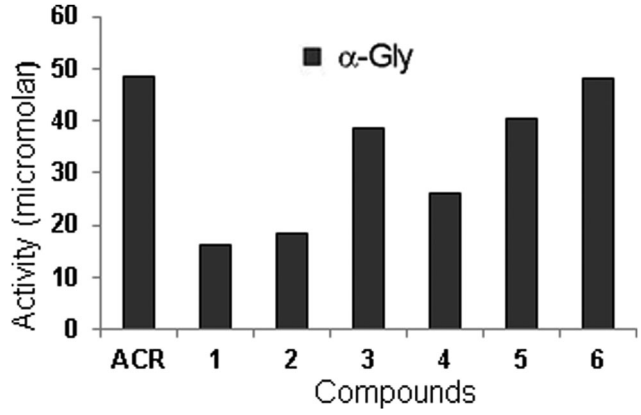

Figure 4. K_i values for α-Gly enzyme.

energy levels of the molecules indicates the molecules' ability to donate electrons. If one of the molecules has a higher HOMO energy level, that molecule can more easily donate electrons (Tüzün, 2020). It should be known very well that the chemical activity of the molecule that can easily donate electrons is higher. On the other hand, another parameter is the LUMO energy levels of the molecules. If one of the molecules has a lower LUMO energy level, that molecule gets electrons more easily. It should be well known that the more easily absorbed electron molecule has higher chemical activity (Akkoç et al., 2020). Many parameters have been obtained as a result of the calculations. It is seen that the numerical values of these parameters are calculated from the numerical value of the HOMO and LUMO energy values. Accordingly, all calculated parameters are given in Table 2.

Many parameters were calculated as a result of the calculations. Afterward, the figural representation of some parameters is given in Figure 5. In the first picture, the optimized structures of the ligand and its metal complexes are given. The next picture shows which atoms the HOMO energy orbitals of the molecule are on. The next picture shows which atoms the molecule has the LUMO orbitals on, the last picture shows the electrostatic potentials (ESP) of the molecule.

When the numerical values obtained in the comparison of the chemical activities of the ligand and its metal complexes are examined, it is seen that the chemical activity of the metal complexes is higher than the ligand molecules. According to the calculations made in both HF and B3LYP

Table 2. The calculated quantum chemical parameters of molecules.

	E_{HOMO}	E_{LUMO}	I	A	ΔE	η	σ	χ	Pİ	ω	ε	Dipol	Energy
HF/6-31g level													
1	−8.7230	1.4447	8.7230	−1.4447	10.1676	5.0838	0.1967	3.6391	−3.6391	1.3025	0.7678	7.6598	−27,147.5168
2	−5.5370	−0.2302	5.5370	0.2302	5.3068	2.6534	0.3769	2.8836	−2.8836	1.5669	0.6382	5.4044	−156,961.9762
3	−5.4948	−0.5516	5.4948	0.5516	4.9433	2.4716	0.4046	3.0232	−3.0232	1.8489	0.5409	9.5991	−152,377.2958
4	−5.5185	−0.2335	5.5185	0.2335	5.2850	2.6425	0.3784	2.8760	−2.8760	1.5650	0.6390	4.9650	−149,590.7088
5	−7.6584	0.4621	7.6584	−0.4621	8.1205	4.0602	0.2463	3.5982	−3.5982	1.5944	0.6272	0.4892	−153,160.1002
6	−7.3164	0.9660	7.3164	−0.9660	8.2824	4.1412	0.2415	3.1752	−3.1752	1.2173	0.8215	3.8830	−146,180.9322
B3LYP/6-31g level													
1	−5.7591	−2.1375	5.7591	2.1375	3.6216	1.8108	0.5522	3.9483	−3.9483	4.3044	0.2323	8.0756	−27,319.4006
2	−4.9201	−2.7642	4.9201	2.7642	2.1560	1.0780	0.9277	3.8421	−3.8421	6.8470	0.1460	2.3830	−157,696.8098
3	−4.9136	−3.5449	4.9136	3.5449	1.3687	0.6844	1.4612	4.2292	−4.2292	13.0677	0.0765	5.9630	−153,123.9210
4	−4.9343	−2.7242	4.9343	2.7242	2.2101	1.1051	0.9049	3.8292	−3.8292	6.6344	0.1507	2.4391	−150,323.8984
5	−5.0524	−2.8262	5.0524	2.8262	2.2262	1.1131	0.8984	3.9393	−3.9393	6.9707	0.1435	1.6953	−153,897.7469
6	−4.9294	−2.7737	4.9294	2.7737	2.1557	1.0779	0.9278	3.8515	−3.8515	6.8814	0.1453	2.4839	−146,908.1341

base sets according to the HOMO energy value of the molecule with the highest chemical activity among the metal complexes, it is seen that the chemical activity of the Mn metal complex is higher than the others. On the other hand, according to the LUMO energy value, the manganese phthalocyanine metal complex (**3**) has higher chemical activity than others.

As a result of molecular docking calculations, the ligand and its metal complexes were used to compare biological activities against enzymes. Two different enzymes were used in the calculations. The most important factor in the process of comparing the biological activities of the ligand and its metal complexes is the interactions between molecules and proteins of enzymes. It should be well known that as these interactions increase, the biological activities of molecules increase. It is known that there are many chemical interactions between molecules and enzymes. These interactions are hydrogen bonds, polar and hydrophobic interactions, π–π, and halogen bonds. The results of molecular docking calculations of the ligand and its metal complexes against enzymes are given in Table 3. The interactions of molecules with the highest biological activity with enzymes are given in Figure 6. A demonstration of the interactions of the other ligand and its metal complexes with enzymes is given in supply Figure 1.

Biological activities of the ligand and its metal complexes were compared in molecular docking calculations. The numerical value of the *E* total parameter obtained as a result of the calculations shows that the molecule with the most negative numerical value of the *E* total parameter used to compare the biological activities of the ligand and its metal complexes has the highest biological activity. The most important factor affecting the numerical value of this parameter is the interaction between molecules and proteins. As this interaction increases, the numerical value of this parameter decreases. The numerical value of this parameter indicates that the interaction of the most negative molecule is higher than the others. The numerical value of the *E* total parameter, which consists of the interaction between ligand and the α-Gly enzyme, is −532.15. This value is the most negative value for this parameter. On the other hand, the numerical value of the *E* total parameter, which consists of the interaction between the ligand molecule and the AChE enzyme, is −120.72. When the molecular docking pictures obtained are examined, the numerical value of the *E* total parameter of the molecules showing horizontal interaction as much as possible is more negative since the surface area of the metal complexes is large. Molecules with more vertical interaction have a lower numerical value of this parameter. Besides, the protein-ligand interaction profiler (PLIP) has been studied in detail due to differences in the energy values of the interactions between proteins and compounds of the studied enzymes. With these calculations, these interactions, such as hydrophobic interactions, hydrogen bonds, and water bridges, show the interaction distance, interaction angle, and with which protein these interactions occur. The interaction of the ligand (**1**) and its metal complex (**3**) of the studied AChE and α-Gly enzymes are calculated PLIP result page are given in Figure 7, supporting material Figures S7 and S8. These figures are given an interaction diagram and table with interaction data for each binding site.

Figure 7 demonstrates the interaction for typical analysis for docking calculation. Protein-ligand interaction profiler for each binding site with ligand and metal complexes provides 2D and 3D interaction diagrams that contain the interaction of metal complexes of the ligand with enzymes (Salentin et al., 2015). As a result of protein-ligand interaction profiler (PLIP) calculations, the interactions of the ligand (**1**) and its metal complexes with enzymes, such as hydrophobic interactions, hydrogen bonds, and water bridges, are given in supporting material Figures S7 and S8. These calculations have been made to examine the interactions that occur in molecules with the highest activity by molecular docking calculations.

4. Conclusion

Herewith, the preparation, spectral characterization, α-glycosidase and acetylcholinesterase enzyme inhibition properties of novel peripherally triazole substituted metallophthalocyanine complexes are presented. The substitution of 1,2,3-triazole groups benefits a remarkable solubility and redshift of the phthalocyanines Q-band. The results have documented that all compounds (**1–6**) have shown the inhibitory effects of α-glycosidase and acetylcholinesterase. Also, in theoretical calculations, both the calculations made with the Gaussian program and the molecular docking calculations, the biological and chemical activities of the molecules were

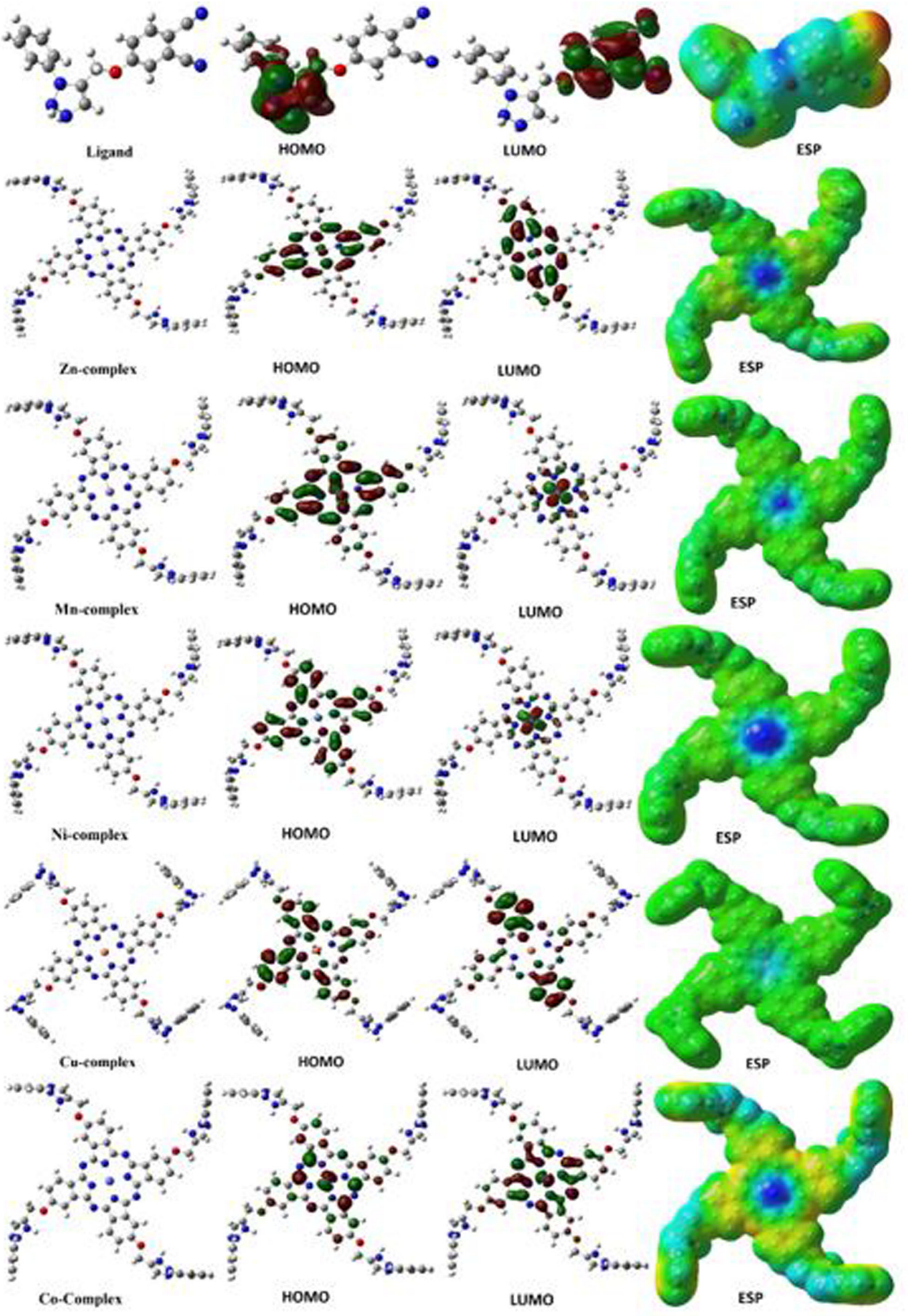

Figure 5. Representations of optimized structures, HOMO, LUMO, and ESP of the ligand (**1**) and its metal complexes (**2**–**6**).

Table 3. Molecular docking E_{total} energy value for studies molecule.

	Protein	
Molecule	α-Gly	AChE
1	−532.15	−120.72
2	−493.13	−231.98
3	−475.42	−233.99
4	−482.70	−218.75
5	−529.23	−207.70
6	−480.67	−232.08

compared. As a result of the comparison made with the numerical values of the parameters obtained by the Gaussian program, it is the manganese phthalocyanine complex with the highest chemical activity. On the other hand, as a result of molecular docking calculations, the molecule with the most negative *E* total parameter interacting most is the manganese phthalocyanine complex. To sum up, molecular docking studies were carried out for the effective-

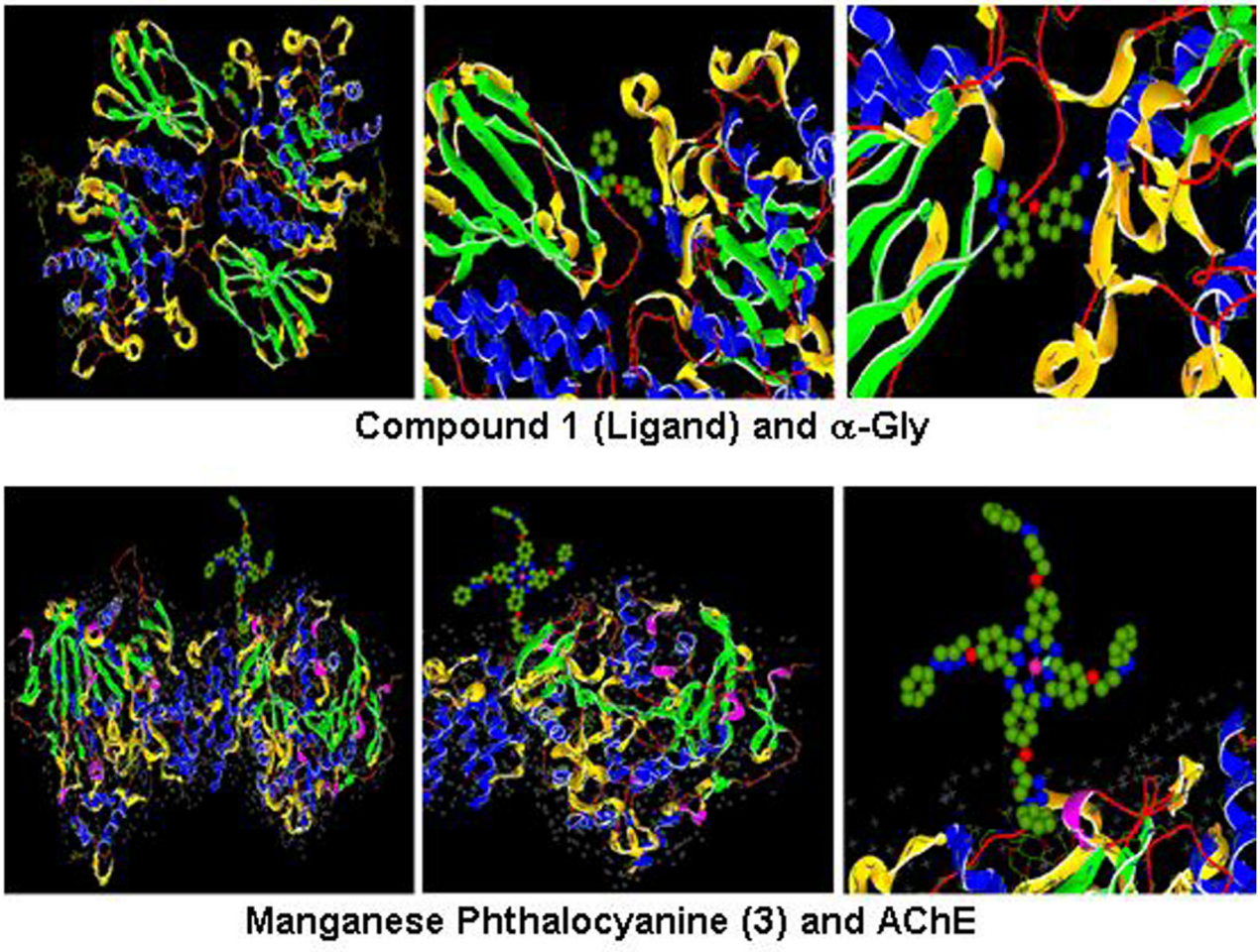

Figure 6. Representation of the interaction of compound 1 and its manganese metal complex with α-Gly and AChE enzymes.

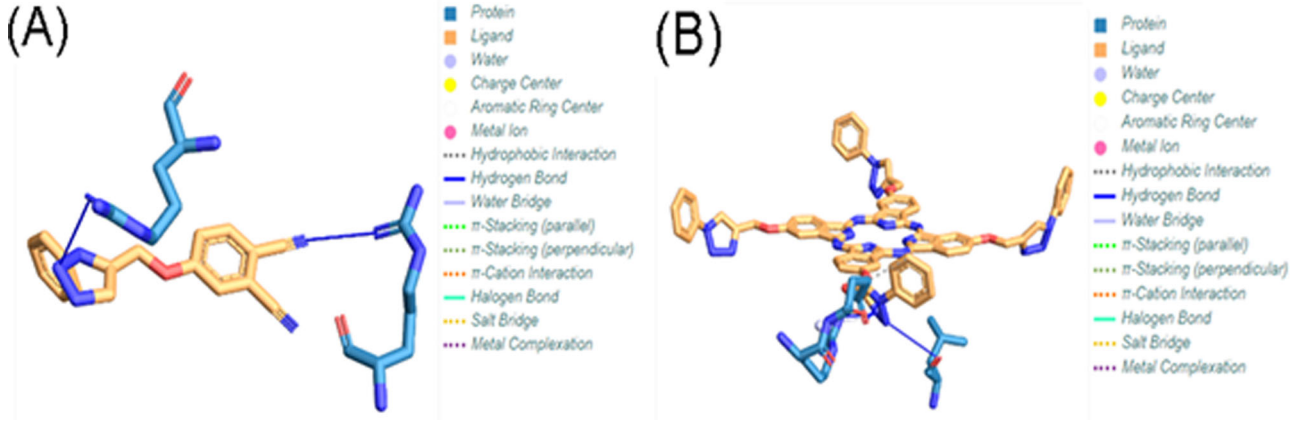

Figure 7. Representation of the interaction of compound **1** with AChE enzymes (A) and manganese metal complex (**3**) with α-Gly enzymes (B).

ness of AChE and α-gly enzyme inhibition of the synthesized compounds, and the calculated results were found to be quite compatible with the experimental data. Finally, by making PLIP calculations, many properties such as the type, distance and angle of the interaction between molecules and enzyme proteins were determined. As a result, these triazole substituted compounds stand out as promising candidates for further studies and novel efficient inhibitors for anticholinesterase and antidiabetic enzymes.

Disclosure statement

There is no conflict of interest.

Funding

This work was supported by Research Fund of the Sakarya University of Applied Sciences (Project Number: 2020-01-10-015) and TÜBİTAK ULAKBİM High Performance and Grid Computing Center (TR-Grid e-Infrastructure).

ORCID

Ümit M. Koçyiğit http://orcid.org/0000-0001-8710-2912
Parham Taslimi http://orcid.org/0000-0002-3171-0633
Burak Tüzün http://orcid.org/0000-0002-0420-2043
Emre Güzel http://orcid.org/0000-0002-1142-3936

References

Agalave, S. G., Maujan, S. R., & Pore, V. S. (2011). Click chemistry: 1,2,3-triazoles as pharmacophores. Chemistry, *An Asian Journal*, *6*(10), 2696–2718. https://doi.org/10.1002/asia.201100432

Akbaba, Y., Türkeş, C., Polat, L., Söyüt, H., Sahin, E., Menzek, A., Göksu, S., & Beydemir, S. (2013). Synthesis and paroxonase activities of novel bromophenols. *Journal of Enzyme Inhibition and Medicinal Chemistry*, *28*(5), 1073–1079. https://doi.org/10.3109/14756366.2012.715287

Akkoç, S., Tüzün, B., İlhan, İÖ., & Akkurt, M. (2020). Investigation of structural, spectral, electronic, and biological properties of 1,3-disubstituted benzimidazole derivatives. Journal *of Molecular Structure*, *1219*, 128582. https://doi.org/10.1016/j.molstruc.2020.128582

Arslan, T., Buğrahan Ceylan, M., Baş, H., Biyiklioglu, Z., & Senturk, M. (2019a). Design, synthesis, characterization of peripherally tetra-pyridine-triazole-substituted phthalocyanines and their inhibitory effects on cholinesterases (AChE/BChE) and carbonic anhydrases (hCA I, II and IX). *Dalton Transactions (Cambridge, England: 2003)*, *49*(1), 203–209. https://doi.org/10.1039/c9dt03897c

Arslan, T., Çakır, N., Keleş, T., Biyiklioglu, Z., & Senturk, M. (2019b). Triazole substituted metal-free, metallo-phthalocyanines and their water soluble derivatives as potential cholinesterases inhibitors: Design, synthesis and in vitro inhibition study. *Bioorganic Chemistry*, *90*, 103100. https://doi.org/10.1016/j.bioorg.2019.103100

Bal, S., Kaya, R., Gök, Y., Taslimi, P., Aktaş, A., Karaman, M., & Gülçin, İ. (2020). Novel 2-methylimidazolium salts: Synthesis, characterization, molecular docking, and carbonic anhydrase and acetylcholinesterase inhibitory properties. *Bioorganic Chemistry*, *94*, 103468. https://doi.org/10.1016/j.bioorg.2019.103468

Becke, A. D. (1988). Density-functional exchange-energy approximation with correct asymptotic behavior. Physical Review A General Physics, *38*(6), 3098–3100. https://doi.org/10.1103/physreva.38.3098

Beduoğlu, A., Sevim, A. M., Koca, A., Altındal, A., & Altuntaş Bayır, Z. (2020). Thiazole-substituted non-symmetrical metallophthalocyanines: Synthesis, characterization, electrochemical and heavy metal ion sensing properties. *New Journal of Chemistry*, *44*(14), 5201–5210. https://doi.org/10.1039/D0NJ00466A

Bitmez, Ş., Sayin, K., Avar, B., Köse, M., Kayraldız, A., & Kurtoğlu, M. (2014). Preparation, spectral, X-ray powder diffraction and computational studies and genotoxic properties of new azo-azomethine metal chelates. Journal *of Molecular Structure.*, *1076*, 213–226. https://doi.org/10.1016/j.molstruc.2014.07.005

Boztaş, M., Çetinkaya, Y., Topal, M., Gülçin, I., Menzek, A., Şahin, E., Tanc, M., & Supuran, C. T. (2015). Synthesis and carbonic anhydrase isoenzymes I, II, IX, and XII inhibitory effects of dimethoxybromophenol derivatives incorporating cyclopropane moieties. *Journal of Medicinal Chemistry*, *58*(2), 640–650. https://doi.org/10.1021/jm501573b

Bulut, N., Kocyigit, U. M., Gecibesler, I. H., Dastan, T., Karci, H., Taslimi, P., Durna Dastan, S., Gulcin, I., & Cetin, A. (2018). Synthesis of some novel pyridine compounds containing bis-1,2,4-triazole/thiosemicarbazide moiety and investigation of their antioxidant properties, carbonic anhydrase, and acetylcholinesterase enzymes inhibition profiles. *Journal of Biochemical and Molecular Toxicology*, *32*(1), e22006. https://doi.org/10.1002/jbt.22006

Bursal, E., Taslimi, P., Gören, A. C., & Gülçin, İ. (2020). Assessments of anticholinergic, antidiabetic, antioxidant activities and phenolic content of *Stachys annua*. Biocatalysis *and Agricultural Biotechnology*, *28*, 101711. https://doi.org/10.1016/j.bcab.2020.101711

Cheung, J., Gary, E. N., Shiomi, K., & Rosenberry, T. L. (2013). Structures of human acetylcholinesterase bound to dihydrotanshinone I and territrem B show peripheral site flexibility. *ACS Medicinal Chemistry Letters*, *4*(11), 1091–1096. https://doi.org/10.1021/ml400304w

Dalvie, D. K., Kalgutkar, A. S., Khojasteh-Bakht, S. C., Obach, R. S., & O'Donnell, J. P. (2002). Biotransformation reactions of five-membered aromatic heterocyclic rings. *Chemical Research in Toxicology*, *15*(3), 269–293. https://doi.org/10.1021/tx015574b

DeLano, W. L. (2002). Pymol: An open-source molecular graphics tool. *CCP4 Newsletter on Protein Crystallography*, *40*, 82–92.

Demir, Y., Taslimi, P., Koçyiğit, Ü. M., Akkuş, M., Özaslan, M. S., Duran, H. E., Budak, Y., Tüzün, B., Gürdere, M. B., Ceylan, M., Taysi, S., Gülçin, İ., & Beydemir, Ş. (2020). Determination of the inhibition profiles of pyrazolyl–thiazole derivatives against aldose reductase and α-glycosidase and molecular docking studies. *Archiv der Pharmazie (Weinheim)*, *353*(12). https://doi.org/10.1002/ardp.202000118

Ellman, G. L., Courtney, K. D., Andres, V., & Feather-Stone, R. M. (1961). A new and rapid colorimetric determination of acetylcholinesterase activity. *Biochemical Pharmacology*, *7*, 88–95 https://doi. org/10.1016/0006-2952(61)90145-9 https://doi.org/10.1016/0006-2952(61)90145-9

Erdemir, F., Celepci, D. B., Aktaş, A., Gök, Y., Kaya, R., Taslimi, P., Demir, Y., & Gulçin, İ. (2019). Novel 2-aminopyridine liganded Pd(II) N-heterocyclic carbene complexes: Synthesis, characterization, crystal structure and bioactivity properties. *Bioorganic Chemistry*, *91*, 103134. https://doi.org/10.1016/j.bioorg.2019.103134

Frisch, M. J., Trucks, G. W., Schlegel, H. B., Scuseria, G. E., Robb, M. A., Cheeseman, J. R., Scalmani, G., Barone, V., Mennucci, B., Petersson, G. A., Nakatsuji, H., Caricato, M., Li, X., Hratchian, H. P., Izmaylov, A. F., Bloino, J., Zheng, G., Sonnenberg, J. L., Hada, M., Ehara, M. … Fox, D. J. (2009). Gaussian 09, revision D.01. Gaussian Inc.

Garman, S. C., & Garboczi, D. N. (2004). The molecular defect leading to Fabry disease: Structure of human alpha-galactosidase. Journal of Molecular Biology, *337*(2), 319–335. https://doi.org/10.1016/j.jmb.2004.01.035

Genc Bilgicli, H., Ergon, D., Taslimi, P., Tüzün, B., Akyazı Kuru, İ., Zengin, M., & Gülçin, İ. (2020). Novel propanolamine derivatives attached to 2-metoxifenol moiety: Synthesis, characterization, biological properties, and molecular docking studies. *Bioorganic Chemistry*, *101*, 103969 https://doi.org/10.1016/j.bioorg.2020.103969

Gülçin, İ., Trofimov, B., Kaya, R., Taslimi, P., Sobenina, L., Schmidt, E., Petrova, O., Malysheva, S., Gusarova, N., Farzaliyev, V., Sujayev, A., Alwasel, S., & Supuran, C. T. (2020). Synthesis of nitrogen, phosphorus, selenium and sulfur-containing heterocyclic compounds - Determination of their carbonic anhydrase, acetylcholinesterase, butyrylcholinesterase and α-glycosidase inhibition properties. *Bioorganic Chemistry*, *103*, 104171. https://doi.org/10.1016/j.bioorg.2020.104171

Günsel, A., Bilgiçli, A. T., Tüzün, B., Pişkin, H., Atmaca, G. Y., Erdoğmuş, A., & Yarasir, M. N. (2019). Synthesis of tetra-substituted phthalocyanines bearing 2-(ethyl(m-tolyl)amino)ethanol: Computational and photophysicochemical studies. Journal *of Photochemistry and Photobiology* A: *Chemistry*, *373*, 77–86. https://doi.org/10.1016/j.jphotochem.2018.12.038

Güzel, E. (2019). Dual-purpose zinc and silicon complexes of 1,2,3-triazole group substituted phthalocyanine photosensitizers: Synthesis and evaluation of photophysical, singlet oxygen generation, electrochemical and photovoltaic properties. *RSC Advances*, *9*(19), 10854–10864. https://doi.org/10.1039/C8RA10665G

Güzel, E., Atsay, A., Nalbantoglu, S., Şaki, N., Dogan, A. L., Gül, A., & Koçak, M. B. (2013). Synthesis, characterization and photodynamic activity of a new amphiphilic zinc phthalocyanine. Dyes *and Pigments*, *97*(1), 238–243. https://doi.org/10.1016/j.dyepig.2012.12.027

Güzel, E., Güney, S., & Kandaz, M. (2015). One pot reaction and three type products; 1(4),8(11)-15(18),22(25) adjacent azine attached as macrocyclically mono, bunk-type (dimer) and polymeric metallo phthalocyanines; synthesis, spectroscopy, and electrochemistry. Dyes *and Pigments*, *113*, 416–425. https://doi.org/10.1016/j.dyepig.2014.08.019

Güzel, E., Günsel, A., Tüzün, B., Atmaca, G. Y., Bilgiçli, A. T., Erdoğmuş, A., & Yarasir, M. N. (2019a). Synthesis of tetra-substituted metallophthalocyanines: Spectral, structural, computational studies and investigation of their photophysical and photochemical properties. Polyhedron, *158*, 316–324. https://doi.org/10.1016/j.poly.2018.10.072

Güzel, E., Koca, A., & Koçak, M. B. (2017). Anionic water-soluble sulfonated phthalocyanines: Microwave-assisted synthesis, aggregation behaviours, electrochemical and in-situ spectroelectrochemical characterisation. Supramolecular *Chemistry*., *29*(7), 536–546. https://doi.org/10.1080/10610278.2017.1288232

Güzel, E., Orman, E. B., Köksoy, B., Çelikbıçak, Ö., Bulut, M., & Özkaya, A. R. (2019b). Comparative electrochemistry and electrochromic application of novel binuclear double-decker rare earth metal phthalocyanines bearing 4-(hydroxyethyl)phenoxy moieties. *Journal of the Electrochemical Society*, *166*(10), H438–H451. https://doi.org/10.1149/2.0511910jes

Güzel, E., Yarasir, M. N., & Özkaya, A. R. (2020). Low symmetry solitaire- and trans-functional porphyrazine/phthalocyanine hybrid complexes: Synthesis, isolation, characterization, and electrochemical and in-situ spectroelectrochemical properties. Synthetic *Metals*, *262*, 116331. https://doi.org/10.1016/j.synthmet.2020.116331

He, Z.-X., Zhou, Z.-W., Yang, Y., Yang, T., Pan, S.-Y., Qiu, J.-X., & Zhou, S.-F. (2015). Overview of clinically approved oral antidiabetic agents for the treatment of type 2 diabetes mellitus. Clinical and Experimental Pharmacology and Physiology, *42*(2), 125–138. https://doi.org/10.1111/1440-1681.12332

Hohenstein, E. G., Chill, S. T., & Sherrill, C. D. (2008). Assessment of the performance of the M05#2X and M06#2X exchange correlation functionals for noncovalent interactions in biomolecules. Journal *of Chemical Theory and Computation*., *4*, 1996–2000. https://doi.org/10.1021/ct800308k

Ismail, M. M., Kamel, M. M., Mohamed, L. W., & Faggal, S. I. (2012). Synthesis of new indole derivatives structurally related to donepezil and their biological evaluation as acetylcholinesterase inhibitors. *Molecules (Basel, Switzerland)*, *17*(5), 4811–4823. https://doi.org/10.3390/molecules17054811

Jiang, Y., Lu, Y., Lv, X., Han, D., Zhang, Q., Niu, L., & Chen, W. (2013). Enhanced catalytic performance of Pt-free iron phthalocyanine by graphene support for efficient oxygen reduction reaction. *ACS Catalysis*, *3*(6), 1263–1271. https://doi.org/10.1021/cs4001927

Kantar, G. K., Baltaş, N., Menteşe, E., & Şaşmaz, S. (2015). Microwave-assisted synthesis and investigation of xanthine oxidase inhibition of new phthalonitrile and phthalocyanines containing morpholino substituted 1,2,4-triazole-3-one. Journal *of Organometallic Chemistry*., *787*, 8–13. https://doi.org/10.1016/j.jorganchem.2015.03.033

Kocyigit, U. M., Taslimi, P., Gurses, F., Soylu, S., Durna Dastan, S., & Gulcin, İ. (2018). The effects of wireless electromagnetic fields on the activities of carbonic anhydrase and acetylcholinesterase enzymes in various tissues of rats. *Journal of Biochemical and Molecular Toxicology*, *32*(3), e22031. https://doi.org/10.1002/jbt.22031

Kurtoglu, G., Avar, B., Zengin, H., Kose, M., Sayin, K., & Kurtoglu, M. (2014). A novel azo-azomethine based fluorescent dye and its Co(II) and Cu(II) metal chelates. Journal *of Molecular Liquids*, *200*, 105–114. https://doi.org/10.1016/j.molliq.2014.10.012

Lolak, N., Akocak, S., Türkeş, C., Taslimi, P., Işık, M., Beydemir, Ş., Gülçin, İ., & Durgun, M. (2020). Synthesis, characterization, inhibition effects, and molecular docking studies as acetylcholinesterase, α-glycosidase, and carbonic anhydrase inhibitors of novel benzenesulfonamides incorporating 1,3,5-triazine structural motifs. *Bioorganic Chemistry*, *100*, 103897. https://doi.org/10.1016/j.bioorg.2020.103897

Nas, A., Biyiklioglu, Z., Fandaklı, S., Sarkı, G., Yalazan, H., & Kantekin, H. (2017). Tetra(3-(1,5-diphenyl-4,5-dihydro-1H-pyrazol-3-yl)phenoxy) substituted cobalt, iron and manganese phthalocyanines: Synthesis and electrochemical analysis. *Inorganica Chimica Acta*, *466*, 86–92. https://doi.org/10.1016/j.ica.2017.05.050

Ogbodu, R. O., Nitzsche, B., Ma, A., Atilla, D., Gürek, A. G., & Höpfner, M. (2020). Photodynamic therapy of hepatocellular carcinoma using tetra-triethyleneoxysulfonyl zinc phthalocyanine as photosensitizer. Journal of Photochemistry and Photobiology B, *208*, 111915. https://doi.org/10.1016/j.jphotobiol.2020.111915

Özçeşmeci, İ., Gelir, A., & Gül, A. (2012). Synthesis and photophysical properties phthalocyanine-pyrene dyads. Dyes *and Pigments*, *92*(3), 954–960. https://doi.org/10.1016/j.dyepig.2011.08.013

Ritchie, D. W., & Venkatraman, V. (2010). Ultra-fast FFT protein docking on graphics processors. *Bioinformatics (Oxford, England)*, *26*(19), 2398–2405. https://doi.org/10.1093/bioinformatics/btq444

Salentin, S., Schreiber, S., Haupt, V. J., Adasme, M. F., & Schroeder, M. (2015). PLIP: Fully automated protein-ligand interaction profiler. *Nucleic Acids Research*, *43*(W1), W443–W447. https://doi.org/10.1093/nar/gkv315

Sepehri, N., Mohammadi-Khanaposhtani, M., Asemanipoor, N., Hosseini, S., Biglar, M., Larijani, B., Mahdavi, M., Hamedifar, H., Taslimi, P., Sadeghian, N., & Gulcin, I. (2020). Synthesis, characterization, molecular docking, and biological activities of coumarin–1,2,3-triazole-acetamide hybrid derivatives. *Archiv Der Pharmazie*, *353*(10), 2000109. https://doi.org/10.1002/ardp.202000109

Stephens, P. J., Devlin, F. J., Chabalowski, C. F., & Frisch, M. J. (1994). Ab Initio calculation of vibrational absorption and circular dichroism spectra using density functional force fields. *The Journal of Physical Chemistry*, *98*(45), 11623–11627. https://doi.org/10.1021/j100096a001

Tan, C.-X., Shi, Y.-X., Weng, J.-Q., Liu, X.-H., Li, B.-J., & Zhao, W.-G. (2012). Synthesis and antifungal activity of 1,2,4-triazole derivatives containing cyclopropane moiety. *Letters in Drug Design & Discovery*, *9*, 431–435. https://doi.org/10.2174/157018012799859954

Tao, Y., Zhang, Y., Cheng, Y., & Wang, Y. (2013). Rapid screening and identification of α-glucosidase inhibitors from mulberry leaves using enzyme-immobilized magnetic beads coupled with HPLC/MS and NMR. *Biomedical Chromatography*, *27*(2), 148–155. https://doi.org/10.1002/bmc.2761

Taslimi, P., Akıncıoglu, H., & Gülçin, İ. (2017). Synephrine and phenylephrine act as α-amylase, α-glycosidase, acetylcholinesterase, butyrylcholinesterase, and carbonic anhydrase enzymes inhibitors. *Journal of Biochemical and Molecular Toxicology*, *31*(11), e21973. https://doi.org/10.1002/jbt.21973

Taslimi, P., Kocyigit, U. M., Tüzün, B., & Kirici, M. (2020). Biological effects and molecular docking studies of Catechin 5-O-gallate: Antioxidant, anticholinergics, antiepileptic and antidiabetic potentials. *Journal of Biomolecular Structure and Dynamics*, 1–9. https://doi.org/10.1080/07391102.2020.1840440

Turkan, F., Cetin, A., Taslimi, P., Karaman, M., & Gulçin, İ. (2019). Synthesis, biological evaluation and molecular docking of novel pyrazole derivatives as potent carbonic anhydrase and acetylcholinesterase inhibitors. *Bioorganic Chemistry*, *86*, 420–427. https://doi.org/10.1016/j.bioorg.2019.02.013

Türkan, F., Huyut, Z., Taslimi, P., Huyut, M. T., & Gülçin, İ. (2020). Investigation of the effects of cephalosporin antibiotics on glutathione S-transferase activity in different tissues of rats *in vivo* conditions in order to drug development research. *Drug and Chemical Toxicology*., *43*(4), 423–428. https://doi.org/10.1080/01480545.2018.1497644

Tüzün, B. (2020). Investigation of the molecules obtained from marijuana: computational study of spectral, structural and docking. *Journal of Physical & Theoretical Chemistry (IAU Iran)*, *16*, 59–74.

Seth Horne, W., Maneesh, K., Yadav, C., David Stout, A., & Ghadiri, M. R. (2004). Heterocyclic peptide backbone modifications in an alpha-helical coiled coil . *Journal of the American Chemical Society*, *126*(47), 15366–15367. https://doi.org/10.1021/ja0450408

Wiberg, K. B. (2004). Basis set effects on calculated geometries: 6-311++G** vs. aug-cc-pVDZ. *Journal of Computational Chemistry*, *25*(11), 1342–1346. https://doi.org/10.1002/jcc.20058

Yiğit, M., Yiğit, B., Taslimi, P., Özdemir, İ., Karaman, M., & Gulçin, İ. (2020). Novel amine-functionalized benzimidazolium salts: Synthesis, characterization, bioactivity, and molecular docking studies. Journal of Molecular Structure, *1207*, 127802. https://doi.org/10.1016/j.molstruc.2020.127802

Yıldız, B., Güzel, E., Akyüz, D., Arslan, B. S., Koca, A., & Şener, M. K. (2019). Unsymmetrically pyrazole-3-carboxylic acid substituted phthalocyanine-based photoanodes for use in water splitting photoelectrochemical and dye-sensitized solar cells. Solar Energy, *191*, 654–662. https://doi.org/10.1016/j.solener.2019.09.043